arXiv:1405.1981v1 [cond-mat.mes-hall] 8 May 2014

A single quantum dot as an optical thermometer for mK temperatures

Florian Haupt, Atac Imamoglu, and Martin Kroner

Institute of Quantum Electronics, ETH Zürich, CH-8093 Zurich, Switzerland

(Dated: May 9, 2014)

Abstract

Resonant laser spectroscopy of a negatively charged self-assembled quantum dot is utilized to measure the temperature of a three dimensional fermionic reservoir down to 100mK. With a magnetic field applied to the quantum dot the single charged ground state is split by the Zeeman energy. As the quantum dot is in tunnel contact with a thermal electron reservoir, a thermal occupation of the quantum dot spin states is enforced by co-tunneling processes. Resonant laser induced fluorescence is used in order to measure the thermal quantum dot spin state population.

A recent development in quantum dot (QD) optics is that it is not the QD itself that is subject to research but rather the interaction with its environment [1–4]. The atom-like optical properties and well understood electrical structure makes the QD an ideal probe for exploring the rich physics of higher dimensional fermionic systems. In particular, when it comes to highly correlated electron states formed by a QD and a two-dimensional electron system such as the Kondo effect ([3, 5, 6]), the temperature of the electron system plays a major role and low temperatures on the mK scale, that can only be reached in a dilution refrigerator, are desirable. While the electronic energy scale in a Fermi reservoir is determined by the temperature, the optical transitions of an isolated QD is hardly influenced by the the temperature of the itinerant electrons or that of the lattice. The tight confinement ($\approx$ 30meV) for the electron and hole wave function in the QD, which is much larger than the thermal energy at liquid Helium temperatures (360μeV), leads to negligible thermal excitation. Furthermore, the QD-phonon interaction only becomes relevant for temperatures larger than 15K, as the relevant phonon modes with sizable coupling strength become occupied [7, 8]. Hence, the resonance line width of excitonic transitions in the QD is in principle limited only by the spontaneous emission rate [9]. This stands in stark contrast to transport spectroscopy of electrostatically defined QDs in a GaAs/AlGaAs two-dimensional electron system: there, the width of Coulomb blockade oscillations is governed by the Fermi-Dirac distribution of electronic energies in the leads. Hence, transport spectroscopy provides a highly sensitive and direct way to measure the temperature of a fermionic reservoir in the mK range [10]. However, transport spectroscopy is not always applicable as a thermometer, in particular for optical experiments.

In this letter, we present an all optical approach to measure the temperature of a fermionic reservoir that is tunnel coupled to a QD. We perform resonant laser absorption spectroscopy on the single-charged exciton ground state transitions of a single QD. In this way, we measure the thermal occupation of the QD ground state and obtain the temperature of the fermionic reservoir. We measure reproducibly a temperature of $T \approx 130$mK. Furthermore, this technique allows to study the heating induced by laser fields.

The QD is embedded in a Schottky diode structure which allows for a controlled charging of the QD with individual electrons [12–14]. To this end the QD layer is separated by a 35nm thick tunnel barrier of intrinsic GaAs from a highly n-doped GaAs layer which acts as an electron reservoir. On top of the sample a semitransparent metallic top gate is deposited

in order to apply a voltage with respect to the electron reservoir. In order to obtain the optical spectrum of the QD we scan a narrow band laser across the exciton transition of a single charged QD and record the resonance fluorescence (RF) in reflection [15, 16]. Cross-polarized excitation and detection is used in order to suppress the laser background (Fig. 1 (a)). The collection efficiency is enhanced by a half-hemispherical ZrO_2 solid immersion lens on top of the sample and a distributed Bragg reflector (28 layers) that has been grown below the QD layer (see [17] for details on the sample structure). A typical spectrum, measured on a negatively charged QD with no magnetic field applied, is shown if Fig. 1 (b). We routinely observe a resonance line width $\gamma \approx 1.5\mu e$V.

The sample is mounted in a cryogen-free dilution refrigerator (Bluefors LD250) with a base temperature of 7mK. For free-space optical access to the sample, the cryostat is equipped with optical windows (fused silica) in all radiation shields of the different thermal stages (Fig. 1 (a)). For optimal transmission of the laser and RF photons the windows are anti-reflection coated in the wavelength range $\lambda = 600\text{nm} - 1000\text{nm}$. In order to suppress etaloning, the windows are wedged by 0.5°. With the windows installed the base temperature of the cryostat increases to 11mK, due to the additional heat load, which is measured to be $\approx 1\mu W$. A single aspheric lens objective ($NA = 0.68$) is used to focus the laser onto the sample surface and to collect the back scattered photons that are ported out of the cryostat to be analyzed at room temperature. The sample is mounted on a piezo driven positioner stage (Attocube ANPx101/res (2x), ANPz101/res (1x)) with a resistive position read out. The resistive readout however induces significant heating and is switched off in order to reach the base temperature. To thermalize the sample, we connect it to the base plate via thermal braids (Attocube ATC100). The signal cables for electrical contacting the sample are, for each line individually, thermalized by a second order low pass filter towards the grounded base plate. The slip-stick mode of operation of the positioners requires connector cables with a large frequency bandwidth. Due to the significant capacitance of the piezo actuators ($C \approx 100$nF) low Ohmic wiring, ideally below 2Ω is necessary and hence low pass filtering as for the signal cables is not applicable. Superconductive wiring is used, in order to minimize the heat load and to guarantee the functionality of the positioners at low temperatures. The cryostat is further equipped with a 9T/3T vector magnet.

In order to measure the electron temperature of the back contact we apply a magnetic field parallel to the optical excitation direction (Faraday geometry) which leads to a Zeeman

splitting of the single electron ground state of the QD [14, 18]. Since the QD is tunnel coupled to the back contact the occupation of the two electron spin ground states will correspond to that of a thermal state. We measure this ground state population by performing absorption spectroscopy on the fundamental charged exciton transitions. The wavelength of the laser field determines which QD transition is driven. The projection of the laser polarization onto the polarization vector representing the optical selection rules of the selected QD transition scales the strength of the laser drive and in turn the strength of the absorption signal. The signal strength is further determined by the population of the corresponding ground state. Hence, keeping the laser polarization constant, a change in the absorption signal signifies a change of the ground state population [19]. For small magnetic fields and high temperatures the two electron spin states have equal population and consequently the two resonances will exhibit equal strength (Fig. 1 (c)). In order to ensure the polarization independence of the measurement we choose the laser field to be linearly polarized, while the optical selection rules for the QD exciton transitions are circularly polarized (Fig. 1 (e)). Further, the laser Rabi frequency Ω is small compared to the radiative emission rate of the QD exciton. This corresponds to driving the exciton transition below saturation in the so-called linear regime where the absorption signal depends linearly on the laser power (or the square of the Rabi frequency) [20]. If the Zeeman splitting of the electron ground state exceeds the temperature, the population of the two electron spin states $(\rho_\downarrow, \rho_\uparrow)$ will differ, resulting in different absorption signals as shown in Fig. 1 (d). There, the temperature of the cryostat is $T_{\mathrm{cryo}} = 11\mathrm{mK}$ and the magnetic field is $B = 0.7\mathrm{T}$. The thermal population $\rho_{\downarrow/\uparrow}$ is given by the Fermi-Dirac distribution and the relative amplitudes of the absorption resonances A_{blue} for the high energy transition (corresponding to the spin up ground state) and A_{red} for the low energy transition (corresponding to the spin down ground state) can be written as:

$$\rho_{\downarrow/\uparrow} = \frac{A_{\mathrm{red/blue}}}{A_{\mathrm{red}} + A_{\mathrm{blue}}} = \frac{1}{\exp\left(\pm\frac{g_e \mu_B B}{k_B T}\right) + 1}. \tag{1}$$

Here g_e is the electron g-factor and μ_B and k_B are the Bohr magneton and the Boltzmann constant, respectively. The externally applied magnetic field is given by B and the temperature of the Fermi sea of electrons in the back contact is T.

In Fig. 2 (a), $\rho_{\downarrow/\uparrow}$ is plotted for two different QDs (QD1, QD3) as a function of the magnetic field. By fitting Eq. 1 to the data points we obtain the temperatures T as labeled

in the plot. The electronic g-factors of the QDs ($g_{\mathrm{e,QD1}} = 0.61$,$g_{\mathrm{e,QD3}} = 0.59$) were determined by a two-laser re-pump experiment as described in [21]. As a comparison the inset in Fig. 2 (a) shows $\rho_{\downarrow/\uparrow}$, when the sample is cooled only by the pulse tube cooler ($T_{\mathrm{cryo}} \approx 4K$). Even at magnetic fields up to 8T the amplitude ratio is not changing appreciably at these temperatures and hence the accuracy of this measurement is limited. For a base temperature of $T_{\mathrm{cryo}} = 11\mathrm{mK}$ we find the electron temperature of the sample to be $T \approx (130 \pm 7)\mathrm{mK}$ with a very high accuracy of 5%. However, the measured electron temperature of the samples is more than one order of magnitude higher than the base temperature of the cryostat.

Before discussing the implications of this unexpectedly high measured temperature, we explain the framework of the temperature measurement where several important points need to be considered for an accurate temperature estimate. As discussed before, the thermal occupation of the QD electronic states is imposed by the coupling to the thermal electron system of the back contact. In particular, a fast and efficient thermalization of the QD electron via co-tunneling processes to the electron reservoir has to be guaranteed. At finite magnetic fields in the center of the voltage range of the stable single electron state in the QD (the X^--plateau) the absorption signal vanishes due to optical spin pumping and slow spin relaxation. This is a consequence of the fact that both, exchange with the Fermi sea and hyperfine flip-flop terms are suppressed [22, 23]. However, if the QD electronic state is tuned close to the Fermi level fast co-tunneling [24] will lead to a thermal occupation of states in the QD and the absorption signal is restored. This is sketched in Fig. 2 (b). In order to ensure a thermal state in the QD we have to apply a gate voltage such that the measured resonance signal (of the two transitions combined) becomes similar to the signal measured with no magnetic field applied. In Fig. 2 (c)-(e) the RF counts are color coded as a function of laser energy and gate voltage for several temperatures and magnetic fields. In panel (c) the end of the charge stability plateau of the singly charged QD is shown at $B = 0\mathrm{T}$ and $T_{\mathrm{cryo}} = 11\mathrm{mK}$. The absorption amplitude is constant over the X^--plateau and then drops off when the QD ground state is doubly charged at more positive gate voltages. This abrupt drop of the RF-signal resembles the sharp Fermi-Dirac distribution of the fermionic reservoir of electrons, which is the source for the second electron tunneling into the QD at this voltage. Here, the distribution of occupied states in the back contact is probed by the electron state of the QD whose energy relative to the Fermi energy is given by the electrostatic energy, $E_{\mathrm{el}} = eV_{\mathrm{g}}/\eta$ with the gate voltage V_{g} and the lever arm $\eta = 5$ [25]. The energy resolution is

given by the voltage fluctuations in the sample to be on the order of $\approx 100\mu e$V restricting the lowest measurable temperature to be measured this way to be $\approx$ 1K. [26]. In Fig. 2 (d) the co-tunneling regime is plotted at $B = 1$T and $T_{\mathrm{cryo}} = 4.3$K. The rather smooth decay of the signal strength towards the edges of the co-tunneling regime is due to the large temperature as discussed before. Also, the amplitudes of the two resonances are almost equal at this low magnetic field. At base temperature however, as shown in Fig. 2 (e), the effect of the temperature is striking. For $B = 0.5$T and $T_{\mathrm{cryo}} = 11$mK the voltage range where we find the QD ground state in a thermal state is reduced to one optical line width (limited by the spectral fluctuations) and the blue, high energy transition clearly shows a larger absorption amplitude than the red, low energy transition. In order to obtain a precise reading of the temperature we perform a measurement as shown in Fig. 2 (d) or (e) for each magnetic field. We post-select the spectra in the center of the co-tunneling range leading to a mean value and a standard deviation (data points and error bars in Fig. 2 (a)) for $\rho_{\downarrow/\uparrow}$.

An important prerequisite for the described analysis is that the resonance line shape is not distorted by other influences such as the nuclear spin environment via the dragging effect [27, 28]. In order to circumvent dragging of the QD resonance we scan the laser fast across the resonance so that the rather slow nuclear spin dynamics cannot follow [28]. More precisely, we scan the laser energy with a rate of $\approx 100\mu e$V/s and average over 10 to 20 scans to obtain one spectrum.

From a four level master equation simulation including the co-tunneling mechanism we conclude that the influence of the resonant laser on the ground state population is negligible for realistic parameters. To experimentally verify that fast and efficient spin pumping does not alter the temperature measurement we also performed a measurement in Voigt rather than in Faraday geometry (data not shown). With an applied in-plane magnetic field the spin pumping rate is as fast as the radiative decay rate [29] and about a factor of 200 faster than in Faraday geometry. Still the temperature measurement resulted in similar values as before.

However, the laser power can certainly lead to local heating of the sample, in particular, due to a considerable absorption of the laser light by the metallic top gate. To exclude laser heating we measured the sample temperature for different laser powers on QD3. In Fig. 3 (a) the obtained temperature values are plotted as function of the laser power measured outside the cryostat. We find that for laser powers below 50nW the measured temperature remains

constant at a value of $T = 130$mK. Hence, we can exclude that the laser power is restricting the temperature measurement. For larger laser power, we do indeed observe an increase of the temperature hinting towards laser heating effects. In order to exclude distortion of the temperature measurement by saturation of the exciton transition [20] we performed a control experiment with a second, off-resonant laser. (The two laser experiment was performed on QD2.) While the resonant probe laser remains at a power of 100nW either a red ($\lambda_{\mathrm{red}} = 980$nm) or blue ($\lambda_{\mathrm{red}} = 904$nm) detuned laser was varied in power. The resulting temperature as a function of the off-resonant laser power is shown in Fig. 3 (a) by the red and blue points respectively. This procedure allowed us to measure the local laser induced heating and resulting temperature up to a laser power of 50μW a power which is two orders of magnitude above the saturation power and also larger than the cooling power of the dilution unit ($\sim 8\mu$W) at base temperature. We observe that the heating due to the resonant laser is considerably larger than due to the off-resonant laser, while the blue and red detuned laser have a very similar heating effect. This is remarkable since the blue detuned laser is very close to the excited QD states. Hence, we would have expected stronger heating effect as for the red detuned laser which is further away from most residual absorption transitions. Both lasers however lie beyond the bandwidth of the Bragg-mirror in the sample. This means that the laser light will be transmitted through the sample and finally be absorbed on the sample holder which is very well thermalized. The resonant laser however will be reflected by the mirror and pass through the gate a second time where it can be absorbed again. This does not explain though the large difference between the resonant and the off-resonant laser heating effects which stems most probably from saturation effects. From the similar results for the two off-resonant lasers we can conclude that the most important mechanism for laser induced heating in these cases is the absorption by the gate electrode.

The measurements at low laser power indicate that the electron temperature is not limited by the measurement itself but is rater limited by the imperfect thermal coupling of the sample to the base plate. It has to be said that since the sample has to be movable and hence can not be mounted in close proximity of the cold plate it is not too surprising that a thermal gradient forms across the superstructure of the microscope. The cooling power mediated by the cables, the most significant cooling mechanism for the electron system in the sample at low temperatures, is limited, despite the careful thermalization and electric filtering. To explore these limits we measured the sample temperature for different base temperatures on

QD2. The data is shown in Fig. 3 (b). In order to ensure the independence of the individual measurements of this experiment the data was taken in random order. For temperatures of the base plate below 100mK the measured sample temperature T remains constant at 160mK [30]. Above 100mK the sample temperature starts to increase and approaches the base temperature (indicated by the green line in Fig. 3 (b)). For clarity the inset shows the difference between the sample and the base plate temperature. Since the cooling power of the dilution unit depends strongly on temperature (quadratically at these low temperatures) for increasing temperature and hence increasing cooling power the gradient that forms across the thermal anchoring of the sample, diminishes from 150mK at $T_{\mathrm{cryo}} = 11$mK down to 25mK at $T_{\mathrm{mix}} = 200$mK.

The setup described in this letter allows for free-space laser spectroscopy on a single QD at mK temperatures. In particular the free space optical access allows for a high degree of polarization control and in turn for measurement of the resonance fluorescence of a QD. This allows us not only to perform laser spectroscopy but also to measure the power spectrum of the resonantly scattered photons. It has been proposed that a single QD strongly tunnel-coupled to an electron reservoir, that exhibits Kondo-correlations for weak optical excitations [3], exhibits a non-equilibrium quantum correlated state in the strong optical driving limit [31]. Such a state is expected to alter the power spectrum from the well known Mollow-triplet [32, 33] to a two peak structure with a characteristic power dependence. In order to explore the feasibility to reach a sample temperature lower than the energy scale of the Rabi energy as well as the Kondo temperature, we measured the Rabi energy of the laser from the power broadening as well as directly from the Mollow-triplet. In the inset of Fig. 4 a typical energy resolved resonance fluorescence measurement is shown as a function of the laser detuning of QD2. This way we determined the Rabi energy $\hbar\Omega$ for a strongly driven QD transition as a function of laser power (red data points in Fig. 4). The black data points in Fig. 4 indicate the extracted linewidth from a resonant saturation experiment signifying power broadening [20]. In order to compare the energy scale of the Rabi energy with the temperature, we also plot the thermal energy corresponding to the laser power dependent temperature from Fig. 3 (a). From this comparison it is obvious that for any laser power the Rabi energy is roughly one order of magnitude smaller than the thermal energy. In order to reach a situation where the Rabi energy can be comparable to the thermal energy of the electron reservoir, improvements need to be made to reduce the electron temperature and

the laser induced heating effects at high laser powers. To address the latter, the Schottky structure with the metallic top gate can be replaced by a pin-diode structure. Also, the light matter interaction can be increased by replacing the ZrO_2 SIL with one made from GaAs [34] or using spacial confinement of the light mode [35], which reduces the required laser power to obtain a certain Rabi energy. In order to further reduce the electron temperature the sample structure can be optimized for a lower resistance electrical connection to the Fermi-reservoir.

In conclusion we demonstrated an all optical scheme to measure the electron temperature in a semiconductor down to the mK range. The presented results open new ways for exploring the physics of semiconductor structures at ultra low temperatures by high resolution resonant optical spectroscopy. In particular the ability to measure the resonance fluorescence gives direct access to the power spectrum of a single QD at mK temperatures in a cryogen free dilution refrigerator.

We thank Clemens Rössler, Khaled Karrai and the Bluefors team for discussions and technical support.

[1] K. Karrai, *et al.*, Nature (London) **427**, 135 (2004).

[2] N.A.J.M. Kleemans, *et al.*, Nature Physics **6**, 534 (2010).

[3] C. Latta, *et al.*, Nature (London) **474**, 627 (2011).

[4] F. Haupt, *et al.*, Phys. Rev. B **88**, 161304(R) (2013).

[5] D. Goldhaber-Gordon, *et al.*, Nature, **391**, 156-159 (1998).

[6] S.M. Cronenwett, *et al.*, Science, **281**, 540-544 (1998).

[7] M. Kroner, *et al.*, Phys. Stat. Sol. B **246**, 795 (2009).

[8] P. Borri, *et al.*, Phys. Rev. Lett. **87**, 157401 (2001).

[9] A.V. Kuhlmann, *et al.*, Nature Physics **9**, 570 (2013).

[10] J.P. Pekola, *et al.*, Phys. Rev. Lett. **73**, 2903 (1994).

[11] I. Favero, *et al.*, Phys. Rev. B **75**, 073308 (2007).

[12] H. Drexler, *et al.*, Phys. Rev. Lett. **73**, 2252 (1994).

[13] R.J. Warburton *et al.*, Nature (London) **405**, 926 (2000).

[14] A. Högele *et al.*, Phys. Rev. Lett. **93**, 217401 (2004).

[15] A.N. Vamivakas, *et al.*, Nature Physics **5**, 198 (2009).

[16] P. Fallahi, *et al.*, Phys. Rev. Let. **105**, 257402 (2010).

[17] W.B. Gao, *et al.*, Nature (London) **491**, 426 (2012).

[18] M. Bayer, *et al.*, Phys. Rev. B **65**, 195315 (2002).

[19] A. Högele, *et al.*, Appl. Phys. Lett. **86**, 221905 (2005).

[20] M. Kroner *et al.*, Physica E **40**, 1994 (2008).

[21] M. Kroner *et al.*, Phys. Rev. Lett. **100**, 156803 (2008).

[22] M. Atatüre *et al.*, Science **312**, 551 (2006).

[23] J. Dreiser, *et al.*, Phys. Rev. B **77**, 075317 (2008).

[24] J.M. Smith *et al.*, Phys. Rev. Lett. **94**, 197402 (2005).

[25] S. Seidl, *et al.*, Phys. Rev. B **72**, 195339 (2005).

[26] This energy scale is not to be confused with the optical resolution of the exciton transition where the sensitivity to the electric field is given by the quantum confined Stark effect.

[27] C. Latta, *et al.*, Nature Physics **5**, 407 (2009).

[28] A. Högele, *et al.*, Phys. Rev. Lett. **108**, 197403 (2012).

[29] X. Xu, *et al.*, Phys. Rev. Lett. **99**, 097401 (2007).

[30] The slightly larger temperature compared to other measurements presented here arise from a larger laser power that was used in this experiment.

[31] B. Sbierski, *et al.*, Phys. Rev. Lett. **111**, 157402 (2013).

[32] B. R. Mollow, Phys. Rev. **188**, 1969 (1969).

[33] A. Muller, *et al.*, Phys. Rev. Lett. **101**, 027401 (2008).

[34] A.N. Vamivakas, *et al.*, Nano Lett. **7**, 2892 (2007).

[35] M. P. Bakker, *et al.*, Appl. Phys. Lett. **104**, 151109 (2014).

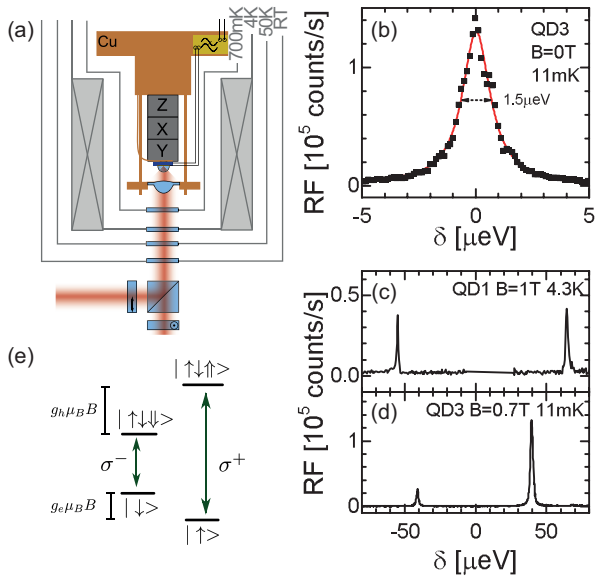

FIG. 1. (a) Schematic of the free-space optical dilution refrigerator. The sample is mounted on xyz-piezo positioner and is in thermal contact with the Cu base plate via thermal braids and the electrical connections. The radiation shields with are labeled by their temperature. The vector magnet is mounted on the 4K stage. Only the room temperature (RT) window is vacuum sealed. The optical excitation and collection are performed via a beam splitter. Two orthogonal polarizing filter are used for the RF experiment as described in the text. (b) Typical RF spectrum as a function of the laser detuning at mK temperature with no magnetic field applied. (c) and (d) RF spectrum vs. laser detuning at different magnetic fields and temperatures as labeled in the figures. (e) Four level scheme of the negatively charged QD with the relevant optical selection rules indicated.

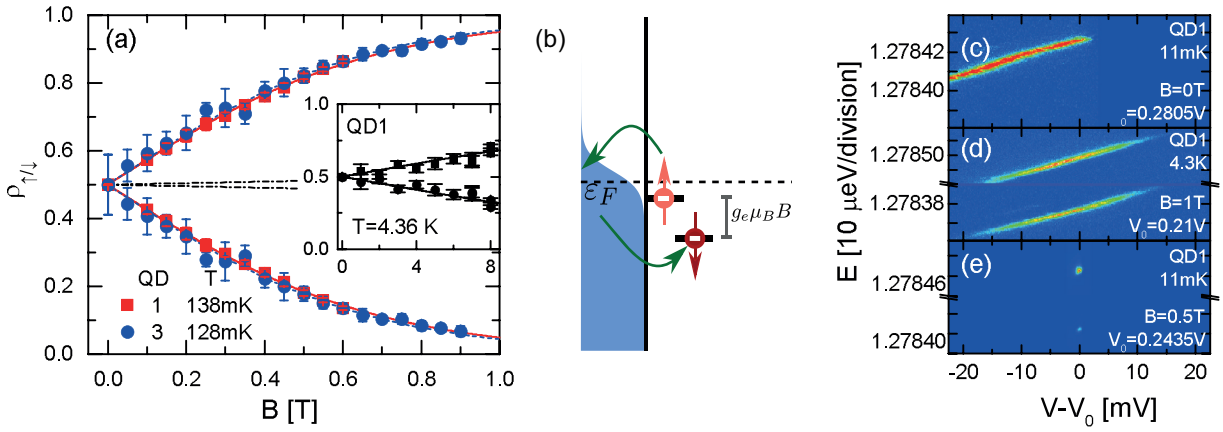

FIG. 2. (a) Relative absorption amplitude of the two optical transitions (as shown in Fig. 1 (c) and (d)) as function of the magnetic field for two different QDs (red squares and blue dots). The correspondingly colored lines indicate the thermal occupation of the QD electronic spin states based on Eq. 1. The inset shows a similar measurement obtained only with the pulse tube cooling (also indicated by the dash-dotted line in the main figure). (b) Schematic to illustrate the co-tunneling process. An electron from the QD (red arrow) can tunnel into the Fermi reservoir (occupation relative to the Fermi energy ϵ_F indicated by the blue area) and be replaced by another electron of opposite spin. The probability of the resulting spin state occupation scales with the Zeeman splitting between the two states. (c)-(e) Color coded RF counts (blue: low counts, red: high counts) as function of laser energy and gate voltage at the edge of the X^--plateau. All measurements where taken on QD1. The magnetic field and temperature are labeled, so is the gate voltage offset V_0 indicating the charging voltage for the second electron. This voltage varies over time and hence is different for these data sets that where taken over the course of several weeks.

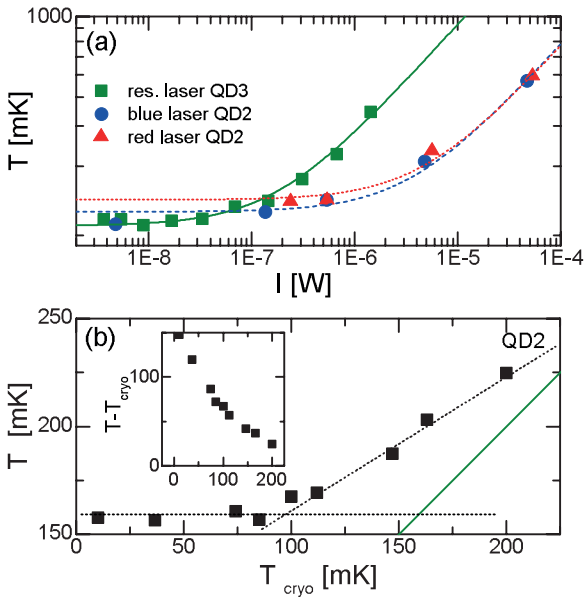

FIG. 3. (a) Measured temperature as a function of the incident laser power. The green squares stand for the experiment with increasing resonant probe laser power measured on QD3. The red and blue data point where acquired for a constant probe laser power ($P = 100$nW) for different red ($\lambda_{\mathrm{red}} = 980$nm) or blue ($\lambda_{\mathrm{blue}} = 904$nm) detuned heating lasers on QD2. The lines are guide to the eyes. (b) Measured temperature T as a function of the mixing chamber temperature T_{cryo} (black squares). The dotted lines are guides to the eye, the green line indicates T_{cryo}. The inset shows $T - T_{\mathrm{cryo}}$ vs. T_{cryo}. This data set was obtained on QD2.

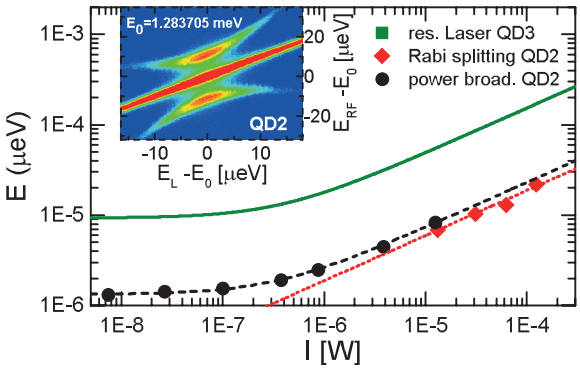

FIG. 4. Power broadening (black dots) of a resonantly driven QD transition and Rabi energy (red diamonds) of the resonant laser driving a QD vs. the corresponding laser power. The dotted and dashed lines are guides to the eye. The green line represents the thermal energy measured as function of laser power as shown in Fig. 3 (b). The inset shows the color coded QD emission as function of the photon energy E_{RF} relative to the QD resonance energy E_0 and the laser detuning from the resonance ($E_{\mathrm{L}} - E_0$). The data was obtained using a scanning Fabry-Perot spectral filter. The splitting at zero laser detuning gives the laser Rabi energy.